

# Data Analysis of a Tethered SpaceMail Experiment

Michiel Kruijff\* and Erik J. van der Heide\*

*Delta-Utec Space Research & Consultancy, 2312 TT Leiden, The Netherlands*  
and

Wubbo J. Ockels†

*Delft University of Technology, 2629 HS Delft, The Netherlands*

DOI: 10.2514/1.41878

The Second Young Engineers' Satellite is a 36 kg student-built experiment that piggybacked on the Foton-M3 microgravity platform in September 2007. Its mission was tethered SpaceMail: a propellantless sample return from an orbital platform. The experiment included a two-stage tether deployment, leading to a swing of the tether toward the local vertical, in which finally a capsule was released from the bottom of the tethered system into a reentry trajectory. The first deployment stage of 3.4 km was completed within about 20 m accuracy. The second stage started on time and the end mass initially accelerated nominally. Then, due to an electrical problem, the tether was deployed to its full length of 31.7 km, rather than to the target length of 30 km. It was nevertheless released at the proper time and at a near-nominal in-plane angle. Data analysis shows that the Second Young Engineers' Satellite scientific objectives were achieved. The two-stage deployment trajectory could be reconstructed and the capsule trajectory could be estimated. The proper performance of the deployer hardware and controller was demonstrated, and tether physical properties were also determined. Finally, simulation and test results could be matched to flight data, providing both confidence and recommendations for preparation of future tether missions.

## Nomenclature

$A$	=	cross-sectional area, m <sup>2</sup>
$A_{\text{sol}}$	=	annulus solidity of the tether spool (fraction of volume containing tether), $(\pi d_{\text{spool}}^2 - \pi d_{\text{core}}^2)/\pi d_{\text{spool}}^2$
$a$	=	speed of sound, m/s
$d$	=	diameter, m
$E$	=	area exponent in the friction brake model, modulus of elasticity, N/m <sup>2</sup>
$F_{\text{brake}}$	=	brake force, N
$f$	=	friction coefficient
$I$	=	inertia multiplier in the friction brake model
$\ell$	=	tether length, m
$m$	=	mass, kg
$n$	=	number of wraps (turns) around the barberpole brake
$P$	=	cyclic period, s
$T$	=	tension, N
$T_0$	=	minimal deployment tension (tether stickiness), N
$t$	=	time, s
$v_0$	=	initial velocity, m/s
$x$	=	coordinate, m
$\theta$	=	in-plane angle, bending angle, rad
$\rho$	=	tether mass per unit length, kg/m
$\sigma$	=	standard deviation
$\Omega$	=	mean angular rate of Foton, $2\pi/5392.3$ rad/s

## I. Introduction

THE Young Engineers' Satellite (YES2) is a 36 kg student-built tether experiment that piggybacked on the Foton-M3 microgravity platform in 2007. It featured the first European space tether deployment and first deployment in over a decade, after a number of

mostly successful orbital missions led by the United States in the 1990s. In 1993 and 1994, two small expendable deployer system experiments (SEDS-I and SEDS-II), each equipped with a 20 km tether, successfully demonstrated an uncontrolled and a controlled deployment, respectively. The tether was drawn from a fixed spool. For additional and controllable friction, it was guided over a capstan tortuous-path braking device referred to as a "barberpole" [1]. Also in 1993, the plasma motor generator demonstrated electrodynamic generation of both power and thrust [2] for the first time. The 4 km tether of the Tether Physics and Survivability experiment tether was deployed passively in 1996. It provided information on long-term damping mechanisms in the tether and robustness of tethers against meteorite and debris impacts [3]. It was reportedly cut only in July 2006.<sup>‡</sup> The TSS1-R conductive tether deployed to 19.6 km from the Space Shuttle in 1996 and demonstrated electron collection principles, generating a significant current in the tether [4]. The YES2 tether deployer, however, is conceptually similar to the much simpler SEDS. The project aimed to continue the SEDS heritage toward a first application by including new challenges for tether control and system design. An important additional boundary constraint came from the educational context in which the project was developed. The YES2 project objectives were threefold: 1) education, 2) deployment of the 31.7 km tether in two stages to accurately release a 6 kg spherical capsule into a reentry trajectory, and 3) landing of the capsule Fotino [5,6] in Kazakhstan. YES2 thus intended to demonstrate SpaceMail, a concept for frequent sample return originally proposed for the International Space Station [7]. A detailed project, design, and mission description can be found in [8]. The project became reality through a comprehensive analysis and testing of the tether system, taking into account safety aspects and critiques right from the start of the project.

The tether was fully deployed on 25 September 2007. Data were collected throughout the mission from various sources and were allowed to achieve the science objectives. The tether deployment was reconstructed and could be cross-validated [9], the tether deployer performance was quantified [10], and tether dynamics could be studied by simulation matching and observing longitudinal, lateral, and spring-mass oscillations [11]. In this paper, a summary of these analyses is provided.

Received 29 October 2008; accepted for publication 7 February 2009.  
Copyright © 2009 by Delta-Utec Space Research & Consultancy, Leiden, The Netherlands. Published by the American Institute of Aeronautics and Astronautics, Inc., with permission. Copies of this paper may be made for personal or internal use, on condition that the copier pay the \$10.00 per-copy fee to the Copyright Clearance Center, Inc., 222 Rosewood Drive, Danvers, MA 01923; include the code 0022-4650/09 and \$10.00 in correspondence with the CCC.

\*Consultant, Middelstegegracht 89G.

†Professor, Department of Aerospace Design, Integration and Operations, Faculty of Aerospace Engineering.

<sup>‡</sup>Data available online at <http://www.satobs.org/noss.html> [retrieved 19 May 2009].

First, however, a project history is provided to give some insight into the peculiarities of the development. Next, the resulting design, mission analysis objectives, and mission results are described in more detail. The results are compared with those of the SEDS missions. The paper concludes with an evaluation of success, problems and solutions, and outlook.

## II. Background

### A. Development

YES2 is a follow-up of the ESA/Dutch YES satellite, launched on Ariane 502 in 1997 [12], which aimed to deploy a 35 km double-strand tether in geostationary transfer orbit. That tether experiment was not performed, for safety reasons. The orbit eventually targeted by the Ariane 502 carrier did not match the original tether mission plan and led to unacceptably risky contingency cases [13]. The YES featured a small expandable deployer system (SEDS) deployer [1]. Because of international traffic in arms regulations, this technology is no longer available for European projects. Through, for example, ESA's Tether System Experiment (TSE) industrial study [14], however, Europe has been initiating development of its own tether deployer system [15] and testing capabilities [16]. Following completion of TSE, a search for safe options for a SpaceMail tether deployment led to the selection of the Foton vehicle in 2001 [17].

The YES2 project was started in 2002 by ESA's Education Office, with education as the primary objective. Apart from the satellite design effort, it also required state-of-the-art technology developments such as the tether system [10], reentry capsule, and novel simulation and software technologies. This made YES2 ESA's most ambitious educational project to date. All ground support and onboard systems were designed and tested by students, and the precise manner of university and student involvement developed with the project.

At the start of the project, a network of 25 universities was set up from Europe and beyond: namely, Canada, Australia, Japan, and Russia. The project management, student guidance, and system engineering was performed by Delta-Utec Space Research & Consultancy (Delta-Utec), a small company in Leiden, The Netherlands. About 250 students worked out initial ideas through group projects [18,19]. A tether mission simulator based on Delta-Utec's tool MTBSim [11] was developed by about 10 students. A tether deployment test rig was developed by about 20 students [20]. The first engineering model of the tether deployer hardware [15] and software was also produced. After the preliminary design review, the design concept was finally fixed in July 2004.

By that time, four centers of expertise had been identified, covering the various domains of the project: mission analysis [Samara State Aerospace University (SSAU)], mechanical engineering (University of Patras), tether system development (Universities of Applied Sciences in Remagen/Krefeld), and testing and reentry capsule development (University of Modena in Reggio Emilia). A fifth group of students was working on system aspects and electronics in Delta-Utec or nearby in ESA's European Space Research and Technology Centre (ESTEC) in Noordwijk.

Most students were only in the project for 3 to 6 months as part of their normal curriculum. They had to be quickly brought up to speed by close guidance and efficient knowledge transfer. Specially developed Web-based system engineering tools were particularly helpful here [21]. Key individuals were kept in the project as long as possible, first through internships and next with short contracts.

Project scope, interface requirements, and budget went through several significant changes, and so creative solutions and compromises had to be found to keep the project going. An example is the reentry capsule concept, which transformed from an inflatable (2003) to a simple passive sphere (2004) to a fully equipped capsule with scientific instrumentation and parachute (2005). Despite the changes, attention for system safety remained a single constant priority. Unlike most student space projects, configuration item control became a requirement, and development was to follow the same analysis, tests, review, and documentation standards as other ESA payloads on Foton. The critical design review was finally completed in the summer of 2006.

The work was then concentrated at Delta-Utec and ESA facilities in which 20 student interns were colocated for an intense final activity. The flight system was delivered to ESA in May 2005, albeit with a tether that was determined to have noncompliant friction characteristics. A newly produced and tested tether was installed in July 2007 in Samara, Russia. At this moment, however, the actual tether mission was still not secured. In late July 2007, a meeting was convened in Moscow between the various interest groups to discuss the safety concerns of the tether deployment with respect to the Foton spacecraft. As a result, it was decided to update the flight software and reroute a number of cables to provide autonomous tether cutting capability, in addition to the already available ground command capability. Agreement for the launch of YES2 was finally obtained in August, when these changes had been implemented and tested. YES2 was launched only weeks later on 14 September 2007.

At this time, over 380 students had participated in the project, from 50 universities in 25 countries. About 180 of them contributed to the project's design documentation, and 100 students performed an internship. The scientific/educational output of the project was about 90 conference papers and 50 thesis reports.

### B. Design

YES2 was built to operate from a Russian platform called Foton-M3, which carries ESA microgravity experiments, among others, under the flag of ESA's Human Spaceflight Department and which orbits at about 265 km altitude. The YES2 was mounted in its entirety on the outside of the Foton-M3 spacecraft (Fig. 1).

The YES2 design, described in detail in [8], includes three components (Fig. 2). Fotino, the 6 kg reentry capsule, contains a science package and a recovery system with a beacon and parachute

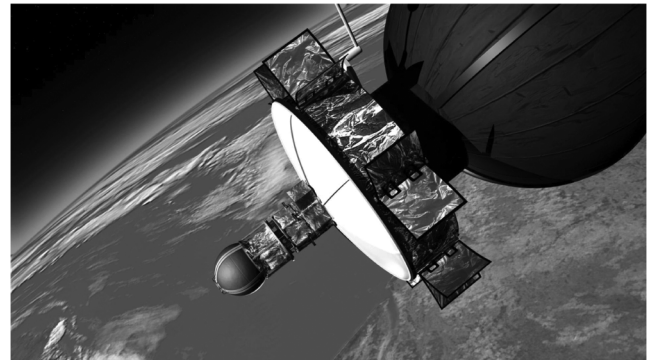


Fig. 1 YES2 on Foton.

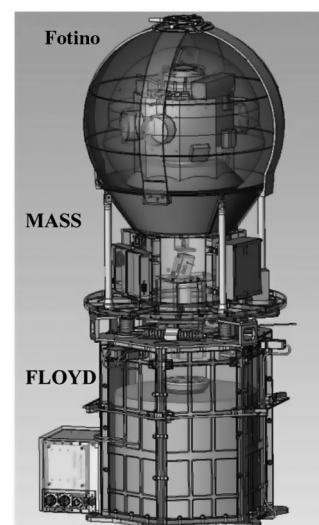
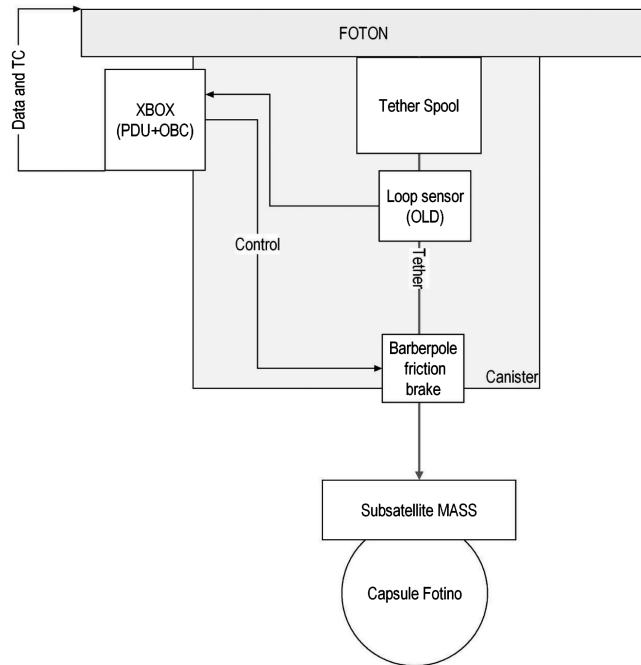


Fig. 2 YES2 contains FLOYD, MASS, and Fotino, the spherical reentry capsule.



**Fig. 3** Simplified overview of the YES2 and tether momentum transfer system.

[22]. It is connected to the tether and released from it by the 8 kg tethered subsatellite Mechanical and Data Acquisition Support System (MASS), which also includes tether science instruments and a transmitter. The tether deployer itself is called FLOYD (Foton Located YES2 Deployer), weighs 22 kg, and remains attached to Foton-M3. It contains the ejection system, the tether deployer, control electronics, and interface to Foton-M3 for power, data storage, telemetry, and telecommand.

Figure 3 provides a simplified schematic overview of the YES2 deployment hardware functionality. The spool has been wound and characterized under controlled conditions before flight [10]. An ejection system initiates the deployment of the tether from this spool fixed and located in FLOYD by ejecting the Fotino/MASS end mass. The tether is unwound as it is pulled over the head of the spool toward a central small exit guide and, for each loop, crosses the optical loop detection (OLD) infrared beams. This allows the OLD electronics to register the passage and forward signals from each of the three encoder channels to the onboard computer (OBC). The OBC filters the signals to generate the length and velocity of deployment. A set of 5 quadratic fits is used (one for each spool part [10]), expressing the unwound number of loops vs the deployed tether length. These fits have an error of about 20 m, or less than 0.1%. Filtered velocity runs about 8 s behind on true velocity. The results are compared with a reference deployment table stored onboard (length and speed versus time); using predetermined feedback gains [23] and a mathematical model of the spool and brake system, commands are sent to the barberpole-brake mechanism to control the deployment by

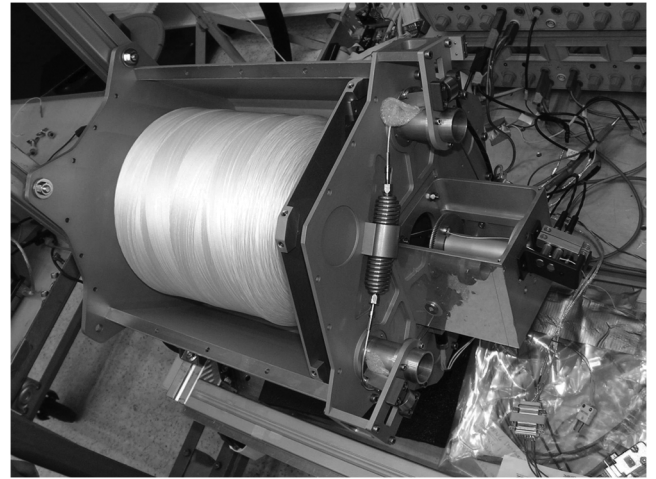


**Fig. 4** YES2 barberpole-brake system in free-deployment configuration (zero wraps around capstan). Also visible are tether cutter bracket, spool and ejection system.

increasing or decreasing friction (Fig. 4) [24,25]. On the barberpole brake [15], the level of friction is controlled by guiding the tether around a central hard-anodized pole of about 2.4 cm diameter. At every control interval of 2 s, the number of wraps  $n$  is adjusted. Even if the tension is significantly different from that expected, only small position adjustments are required: typically less than one-third wrap per control interval. Each wrapping increases the effective friction by a factor of about 3, such that a large range of tension (as typically required for a tether deployment) can be controlled with little effort.

Equation (1) provides the mathematical model that is used to estimate the friction level applied by the brake for each number of wraps  $n$  [26].

$$T = \left( T_0 + I \frac{\rho \dot{\ell}^2}{(1 - A_{\text{sol}}(\ell/\ell_{\text{tot}}))^E} \right) e^{2\pi f(\dot{\ell})n + f_{\text{guides}}(\theta_{\text{guides}} + \theta_{\text{ref}} - \theta_{\text{Foton}})} \quad (1)$$

The model contains the effects of tether stickiness on the spool ( $T_0$ ), tether unwinding dynamic effect (roughly proportional to the deployment speed squared and increasing heavily when deployment approaches the solid core of the spool), and the friction effect of the wrapping of the tether around the pole,  $f$ . The nominal values for the parameters were determined from measurements and tests in a variety of environments [11,15,20] (Table 1). The in-plane angle of the Foton spacecraft main axis,  $\theta_{\text{Foton}}$ , was assumed to be 0 during development. The YES2 team later derived that the Foton vehicle was not nadir-pointed, but was actively controlled to track the tether angle (up to a maximum of 30 deg), and so, in fact,  $\theta_{\text{Foton}} \approx \theta(\text{tether})$ . The acceptable range of the parameters for successful control was determined by simulation. Friction is a rather empirical process, but because of the closed-loop control, only a matching of the model to reality by about a factor 3 was required.

**Table 1** Preflight deployer model parameters

Parameter	Symbol	Preflight value
Tension, N	$T_0$	0.0085
Inertia multiplier	$I$	8
Density, kg/m	$\rho$	0.000182
Annulus solidity	$A_{\text{sol}}$	0.9
Area exponent	$E$	0.73
Friction coefficient	$f$	0.2 above 1.5 m/s deployment speed, decreasing linearly to 0.1 at zero deployment speed
Friction coefficient on guides	$f_{\text{guides}}$	0.184
Bending angle over guides, rad	$\theta_{\text{guides}}$	0.64
In-plane orientation of Foton, rad	$\theta_{\text{Foton}}$	0, assumed

### III. Mission

#### A. Mission Analysis Objectives

The YES2 mission and associated data analysis has a primary science objective to demonstrate a two-stage controlled tether deployment: that is, a partial deployment to the vertical, followed by a hold phase and continued deployment to a large forward angle, followed by a swingback to the vertical, where a payload is released. Such a deployment strategy is designed to maximize robustness against uncertainties [7]. Sensors have been selected to allow detailed reconstruction of the deployment trajectory. An important driver of both the design phase and the mission analysis has also been to demonstrate safety and predictability of the tether deployment and control. The achieved capsule trajectory and projected or actual landing spot are to be determined. The predictability of deployer hardware friction and the possibility to adjust those friction levels in a predictable manner determines the hardware's potential to control the deployment. The hardware performance is thus to be assessed based on recorded tension data and compared with results from ground tests and simulations. Apart from the friction and brake performance, tether properties such as stiffness, speed of sound, and damping are to be derived from the flight data and compared with preflight test results. The closed-loop control software performance in the actual flight situation is also to be evaluated by studying the data from the deployment sensors and the software controller and by correlating the control to the dynamic response of the deployment.

Simulations are to be matched to the flight data and the simulator is to be updated to deal with any discrepancies found. Using the improved simulator, deployer and controller performances are to be combined to update estimates for the SpaceMail landing accuracy obtainable with the YES2 hardware. The validity and limits of simulations and ground tests are to be assessed and recommendations are to be defined for the preparation procedures of future tether missions.

#### B. Data Sources

A variety of sensors are available to track the deployment. As previously explained, the primary sensors are OLD in the tether core on FLOYD. They are the only sensors used for closed-loop control. They provide information on length and rate with which the (postflight) deployment angle and tension can be reconstructed using a simple expression for tether dynamics [Eq. (2) and [9]]. Note that Eq. (2) was used as the first source to reconstruct both in-plane angle  $\theta$  and deployment tension based on the tether length data (from OLD and other sources) [32]:

$$\begin{aligned} \ddot{\theta} + 2\dot{\ell}(\dot{\theta} - \Omega) + \frac{3}{2}\Omega^2 \sin 2\theta = 0 \\ - (m + \rho\ell) \cdot \ddot{\ell} + (m + \frac{1}{2}\rho\ell) \cdot \ell \cdot [(\dot{\theta} - \Omega)^2 \\ - \Omega^2(1 - 3\cos^2\theta)] = T = F_{\text{brake}} + \rho\dot{\ell}^2 \end{aligned} \quad (2)$$

Equation (2) is valid for light tethers with a small end mass deployed from a large platform in circular orbit and takes the shape of Hill's equations expressed in polar coordinates, slightly adapted to include tether tension and tether density aspects. These equations ignore tether flexibility aspects. For this reason, a simulation was made to match the mission data using MTBSim, an advanced tether simulator, such that the influence of these aspects could also be studied [11].

Inside Foton, sensitive three-axis accelerometers and magnetometers operating at 1000 Hz and belonging to the direct measurement of acceleration (DIMAC) payload [27] register the full deployment and allow for an independent derivation of tether tension. The direction of the tether near Foton can be obtained from the  $X$  and  $Y$  components of the disturbing acceleration in Foton's body frame, combined with magnetometer and horizon sensor data on Foton's attitude in space. A spectrograph can be used to determine the deployment rate versus time and to identify the exact time of deployment of a number of points along the length of the tether (based on known changes in the tether's winding pattern). On MASS, magnetometers, a tensiometer, and a gyroscope measure the

subsatellite dynamics and the disturbances created by the ejection and the safety and securing features included in the first 15 m of the tether. The simple data package [28] provides information for a range of 150 m. Housekeeping information such as voltages, temperatures, commanded brake position, error flags, etc., can be used to correlate and verify the measurements. Navigation data [Global Positioning System (GPS) and Global Navigation Satellite System (GLONASS)] of the FLOYD position in space during the tether deployment are also available (YES2 SSAU experiment) [28–30] and allow for in-plane angles and tether length confirmation. These data have not been taken into account for the analysis reported here. An overview of the usage of and accuracy attainable with the sensor data is provided in Appendix A.

#### C. Mission Summary

The mission timeline is summarized in Table 2 and Fig. 5. In this figure, the shaded zones indicate night time. The approximate temperature of the tether on the spool core (OLD) and OBC (control box or XBOX) are also indicated.

On the 11th day of the Foton-M3 mission, the YES2 experiment was switched on and deployed a 31.7-km-long, 0.5-mm-diam mechanical Dyneema® tether in two stages, with a combined duration of 8626 s, downward from the 6535 kg Foton-M3 spacecraft at an altitude of about 265 km. Orbital dynamics (gravity gradient and Coriolis forces) induced buildup of a significant in-plane angle during the final part of deployment. After deployment completion, the tether system behaved as a pendulum and swung back toward the vertical equilibrium position. The tether was then cut as planned at  $t = 9364$  s. By cutting the tether near the vertical (below the deployment platform), an efficient and propellantless momentum transfer between the upper and lower end masses was executed. Such a momentum transfer allows for a number of applications, such as launch assist [31] or, in the case of YES2, deorbit [7]. At the same time, the YES2 deployment included a stabilized stage that many future tether missions will have to go through. In fact, the YES2 two-stage deployment was somewhat more complex than may be required for other applications.

In the YES2 approach, a vertical stage of 3.4 km length is first deployed to stabilize, dampen any transversal oscillations, and synchronize the 13.9 kg end mass with the argument of the target trajectory. In principle, the time after completion of the first stage allows also for fine-tuning of the mission timeline (through ground control) for improved landing accuracy. A much longer second stage with relatively large gravity-gradient forces can then be deployed quickly and robustly (up to the full length of 31.7 km in the case of YES2).

Deployment tension varied between 0.03 N in the first stage to 0.16 N during the hold phase between the two deployment stages and up to 2 N in the second stage. The foreseen maximum tension at the end of the second stage was 3 N, but due to overdeployment, a brief shock of much higher tension was introduced as the end of the tether was reached. This overdeployment was due to an unfortunate failure of an electronic patch becoming apparent about 6200 s into the deployment. It lead to an open-loop completion of deployment, without smooth end-braking and, instead, a peak in tension of about 40 N. The YES2 tether is able to withstand a 300 N shock. A system for passive release of the tether at about 60 N tension shock was implemented for safety [8]. With the end shock level somewhat smaller, it did not trigger, allowing the mission to continue after the deployment completed. In-plane angles during deployment ranged from 0 to 50 deg (forward direction), with a final downward-backward swing from about 40 deg amplitude back toward the vertical. The deployment speed ranged from an initial 2.2 m/s to a maximum 16 m/s and about 15 m/s at the end of deployment (Fig. 6) [9].

The tether dynamics analysis objectives were achieved, although due to the lack of beacon signal from Fotino, the capsule's landing spot could only be estimated. The offnominal ending of the deployment in absence of a smooth end brake allowed only for an indirect demonstration of the SpaceMail potential, but it caused tether



**Table 2** YES2 mission timeline<sup>a</sup>

Event	Time (UTC)	YES2 time (seconds relative to YTK2)	Description
<i>Orbit 1</i>			
Launch Foton	11:00:00	—	14 September 2007
<i>Orbit 163</i>			
Upload telecommand timeline	14:00:00	—	24 September 2007
<i>Orbit 171</i>			
Switch YES2 on	2:03:00	−9813	25 September 2007
First relayed raw data downlink	2:07:00	−9573	Through Telescience Support Unit (data storage and forwarding) inside Foton (confirms temperature OK)
YTK10	2:13:00	−9213	Arm pyros
<i>Orbit 172</i>			
TKTM	3:17:00	−5375	Receive telemetry (confirm arming)
<i>Orbit 173</i>			
YTK8	4:45:33	−60	Switch on MASS
YTK2	4:46:33	0	Ejection
TKTM	4:50:00	207	Receive telemetry (confirm ejection, reaching 300 m safe length)
Start hold phase	5:55:13	4120	—
<i>Orbit 174</i>			
YTK4	6:19:32	5580	Prepare for second stage
Start second stage	6:21:12	5680	—
TKTM	6:23:00	5786	Receive telemetry (confirm first stage and start second stage)
Release Fotino	7:22:17	9344	—
YTK3	7:22:37	9364	Cut tether on Foton side
<i>Orbit 175</i>			
Projected Fotino landing	7:57:00	11,420	Nominal landing site 66.2E 50.6N. Ground recovery team situated downstream at 67.5E 51.6N. No beacon signal was received
TKTM	7:53:00	11,186	Receive telemetry (confirm second-stage deployment)
<i>Orbit 176</i>			
Switch YES2 off	9:16:00	16,166	—
<i>Orbit 178</i>			
Last relayed raw data downlink	12:15:00	—	Through Telescience Support Unit (data storage and forwarding) inside Foton (full download raw data)
<i>Orbit 189</i>			
Landing Foton	~7:58:00	—	26 September

<sup>a</sup>YTK denotes YES2 telecommand and TKTM denotes telemetry telecommand.

dynamics that provided data on complex and pronounced oscillations. Fotino recovery (including measurements made during its reentry) could not yet be achieved, but was explicitly not a project objective.

## D. Mission Results

### 1. Deployment Reconstruction and Fotino Trajectory

The deployment started with ejection of the MASS/Fotino end mass. Analysis of the OLD data and the fit to integrated acceleration measurements from both MASS and DIMAC demonstrate that the (effective) ejection speed was nominal: 2.2 m/s. The pitch-off rate of the capsule could be determined from MASS gyroscope and magnetometer data to be only 1.55 deg/s, demonstrating excellent performance of the 40 J ejection system (Fig. 7). Simulations could

be matched to the end-mass angular dynamics for extrapolation throughout the mission, all the way into reentry.

The OLD data showed nominal unwinding behavior of the tether during most of the first deployment, although there were two periods of irregular unwinding of loops from the spool. The first period lasted for a few minutes and peaked about 30 s after deployment. It is likely that this irregularity was the result of end-mass oscillations, which could not be tested reliably on the ground.

The onboard computer software uses a filter to calculate the velocity from the OLD pulses. As the tether unwinds axially from the spool, it passes the three OLD channels (simply tagged 1, 2, and 3 and mounted in the head of the spool), necessarily subsequently and repetitively in a fixed order: 1-2-3-1-2-3-1, etc. (Fig. 8 and row A in Table 3). The filter algorithm contains two simple checks to verify healthy performance of the OLDs.

The first check verifies whether the pattern of pulses from the three channels arrives in the proper order. If an offnominal order of pulses is recognized (e.g., 1-3-1-2-3), the algorithm assumes that an intermediate pulse is missed (in this case, channel 2), and the software fills in the gap (row B in Table 3). Based on manual inspection of all OLD data, it can be said that this feature performed without problems during the flight.

The second feature is activated in case two subsequent pulses arrive from the same channel (e.g., 1-1-2-3). Such an event is likely to occur if the tether vibrates briefly in front of a single channel (row C in Table 3). This is what the software principally assumes, and in such a case, the noise is ignored. However, if the pulse interval lasts longer than a certain period of time (set based on ground tests), the filter assumes that there was a OLD pulse failure on two subsequent channels (here, channels 2 and 3) (row D in Table 3), and the algorithm fills in the gap by counting a full loop.

Analysis of the raw flight data shows that such a double-channel failure hardly ever occurs, and this additional failure recovery

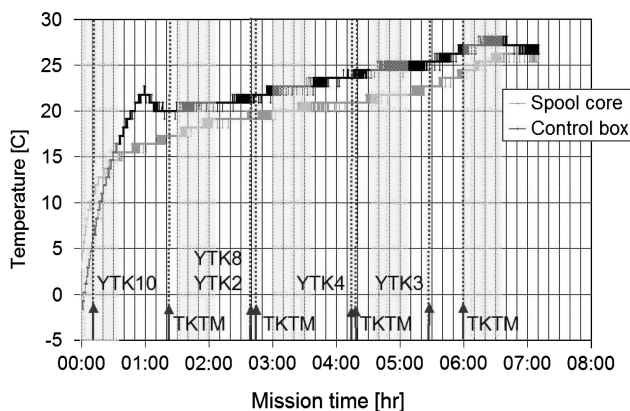


**Fig. 5** Temperature and telecommand history during YES2 mission.

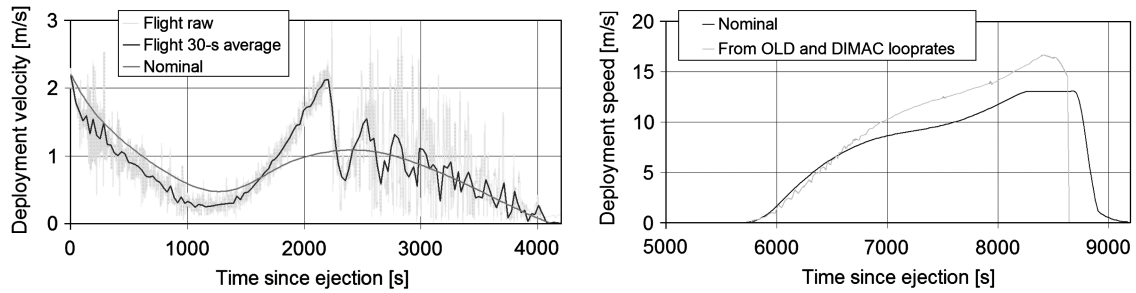


Fig. 6 Deployment speed of YES2 mission flight data vs nominal in first and second stages.

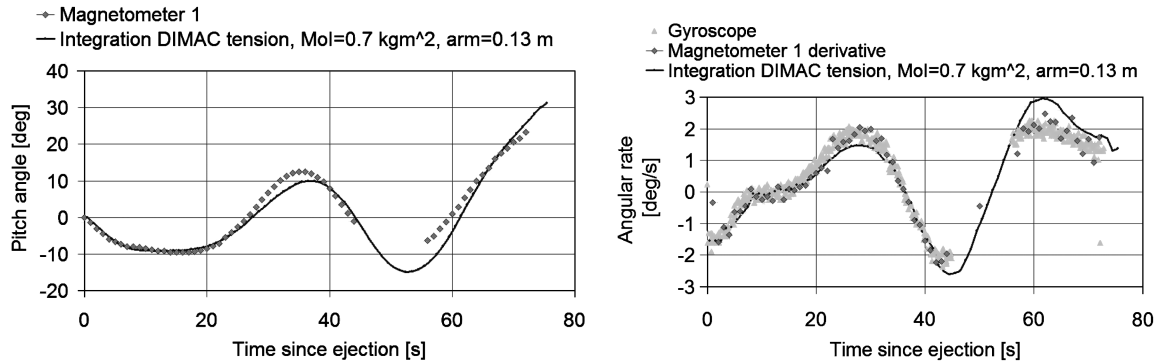


Fig. 7 MASS magnetometer and gyro data directly after ejection, including simulator matching.

function is therefore unnecessary. In fact, during the first period of irregular deployment, the algorithm falsely triggered several times in a row and counted about 10 or so false loops of tether. As a result, the deployment velocity was overestimated by about 10% for tens of seconds, and the controller responded by additional braking (Fig. 9). Note that in this figure, the initial tension spike is due to deployment of a damper system, whereas the stretched second increase in tension is related to the increased number of turns on the barberpole brake. The actual deployment velocity was brought approximately 40 cm/s under the nominal velocity in the first minute after ejection.

This is not normally a problem, but because the tether minimal deployment tension (stickiness to the spool) also turned out to be just outside specifications (about 4 cN compared with the maximum allowable of 3 cN), there was no possibility for smooth control. The brake was released fully for a duration of 2200 s, during which the controller eventually allowed the tether to spool out faster than nominal to catch up with the initial lost length. By the time the length reached the nominal value again, the deployment velocity was significantly higher than nominal and the brake was reapplied abruptly (Fig. 10). A control and speed oscillation started (Fig. 6), leading to a 10 deg or so in-plane oscillation at the end of the first stage (Sec. III.D.3).

The first-stage length that was obtained was nevertheless determined to be very accurate, 3378 rather than the nominal 3390 m, providing a good basis for a nominal second stage of deployment (Fig. 11).

The hold phase was nominal and the length was held constant, with subtle adjustments by the controller that were meant to maintain a minimum amount of brake turns to allow a quick and nominal start of the second stage. The transversal oscillations dampened out for a large part.

Table 3 Typical OLD channel activation sequences

A	Normal	1	2	3	1	2	3
B	One channel failure	1	—	3	1	—	3
C	Isolated tether vibration	1–1	2	3	1	2	3
D	Double-channel failure	1	—	—	1	—	—

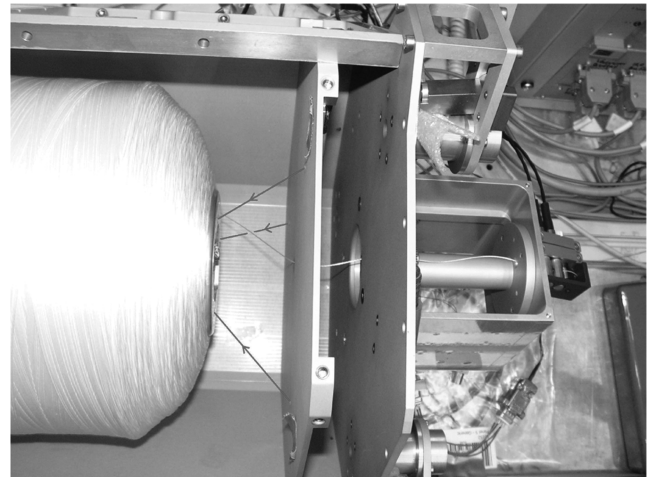


Fig. 8 As the tether unwinds axially from the (fixed) spool to the exit guide, it interrupts three infrared beams sequentially.

Some 500 s into the second stage, the OLD data as recorded by the OBC started to break down due to a failing electronics patch that was intended to correct a broken input signal on the OBC's CPU [24] (Fig. 3). In response, the controller turned the brake to zero and the deployment continued in a free uncontrolled manner. With the brake set to zero, the deployment accelerated somewhat faster than nominal (to 16 m/s, rather than 13 m/s) and overdeployed to the full length of 31.7 km, rather than the target length of 30.0 km. There was no gentle deceleration near the end: the deployment stopped abruptly at about 15 m/s, leaving a distinct tension signature at  $t = 8626$  s.

Despite the incompleteness of the OLD data from 6260 to 8626 s, sufficient data were still available to determine the loop rate to within 1 Hz (about 0.3 m/s) until  $t = 8250$  s (Fig. 12). In this figure, OLD loop rates were determined based on the number of same-channel pulses received within  $\sim 0.2$  s time intervals. As the time of deployment completion was known within 1 s from the tension pulse, the remainder of the deployment could be interpolated with an accuracy of about 1 m/s.

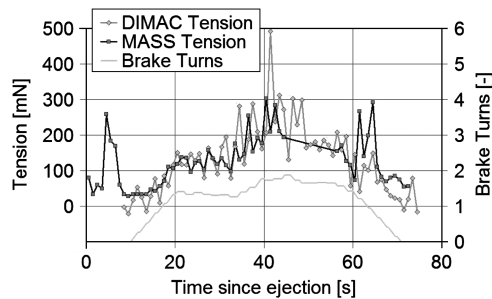


Fig. 9 Tension and braking activity directly after ejection.

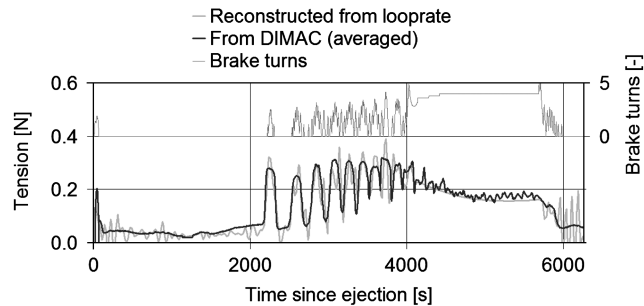


Fig. 10 YES2 flight tension and brake activity from ejection to start of second stage.

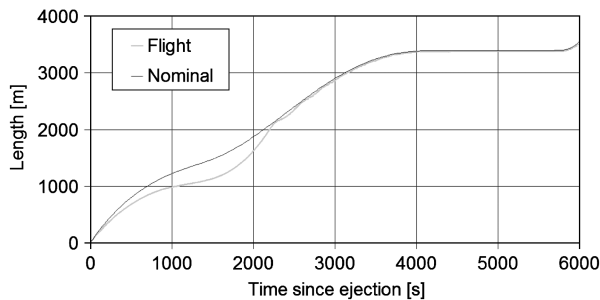


Fig. 11 YES2 deployed length, first stage.

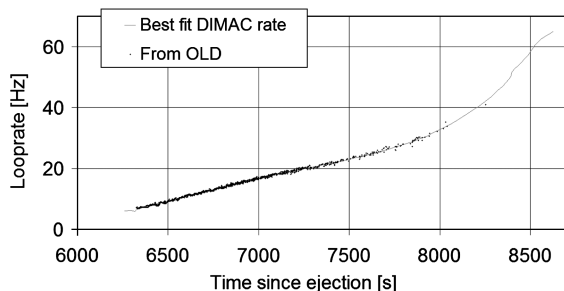


Fig. 12 Loop-rate development during uncontrolled deployment in stage 2.

The result was soon confirmed and further improved to better than 0.7 m/s accuracy with the help of a rather fascinating spectrograph of DIMAC measurements (Fig. 13). The color in this figure shows the intensity of microgravity-disturbing accelerations of the 6535 kg Foton-M3 spacecraft as a function of time (horizontal) and frequency (vertical), obtained through Fourier analysis. Remarkably, the rattling of the unwinding tether (weighing only 0.2 g/m) during most of the second stage of deployment was clearly distinguished by the DIMAC experiment. The tether's disturbance to Foton probably becomes measurable as soon as the deployment velocity becomes sufficiently large to expel the tether by centrifugal force radially from the spool and collide it with the wall of the canister. Note that this figure is a composite of results in the various Foton body axes to

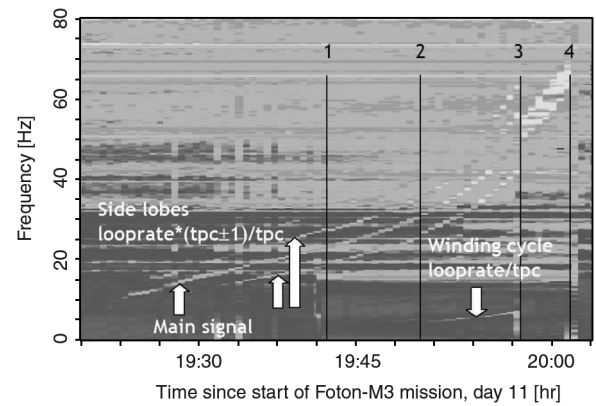


Fig. 13 DIMAC spectrograph with indication of four absolute length markers (see Sec. III.D.1).

maximally highlight the YES2 loop-rate curve. The rate information extracted from this graph fits neatly to the OLD rates (Fig. 12).

Moreover, the spectrograph reveals details of the winding pattern (i.e., settings applied during the preflight tether spool manufacturing), such as the cyclic frequency of the winding head [10] or, in other words, the number of spool turns per winding cycle (tpc in Fig. 13). The cyclic frequency is visible directly, as well as in the form of secondary arms accompanying the main loop-rate signal. On close inspection of the figure, there are a number of discontinuities that relate to the transitions in turns per cycle applied during the winding at lengths known exactly (Fig. 13 and Table 4).

The main curve broadens as soon as the unwinding reaches the parallel part of the spool and the curves indicating the cyclic frequency disappear (marker 3). During parallel winding, all ( $\sim 400$ ) loops within one layer are placed neatly and adjacently from the top to the bottom of the spool and vice versa in the next layer. The top and bottom of the spool do not have the same diameter, however. In fact, the width of the curve beyond marker 3 turns out to exactly represent this conical property of the spool. In the parallel section, about 13% more loops need to unwind per second when the tether is taken from the narrow top of the core than when it is taken from the wider bottom at equal velocity. The unwinding of a full layer between core top and core bottom takes about 7 s at the observed loop rates. The resolution of the spectrograph is about 32 s, sufficient to capture more than four full layers. The width of the curve therefore shows the range within which the loop rate oscillates as the tether unwinds with a rather smoothly developing velocity.

In any case, it is possible to extract from the spectrograph four definite absolute length measurements that turn out to match well with the integrated rate data and provide independent confirmation. The maximum length reconstruction error during the second stage is estimated to be 0.3% or 100 m, limited mostly by the resolution of the spectrograph as provided to the YES2 team.

The development of in-plane angle with time should be determined precisely if the trajectory and projected landing site of the Foton capsule is to be determined. Estimates of the in-plane angle development have so far been made in two ways: through deployment reconstruction using Eq. (2) (or, alternatively, the MTBSim tether simulator) and through the DIMAC three-axis accelerations. The Foton-M3 had the DIMAC  $x$  accelerometer aligned with its body axis (in the approximate direction of the tether deployment), the  $y$  accelerometer in plane, and the  $z$  accelerometer out of plane. The Foton had an active attitude control system during YES2 using cold-gas thrusters, acting mainly in the  $y$  direction, and its activation pulses could be easily recognized in the acceleration data, isolated, and edited out. The angle between Foton-M3 and the tether could then be determined simply by taking the arctangent from the  $y$  and  $x$  measurements. The attitude of Foton itself was obtained mostly from the DIMAC magnetometers, except at in-plane angles above  $\theta = 30$  deg, where the thruster activity was too intense for clean editing. Here, the angle is assumed to be constant, in agreement with Foton horizon sensor data. With these results combined, the tether in-plane

**Table 4** Winding events recognized during deployment by DIMAC instrument

Marker	Winding event	$t$ , s	Length, m	Loops
1	5 to 6 turns per cycle	7512	15,421	24,135
2	6 to 7 turns per cycle	7937	21,168	35,754
3	Crisscross to parallel	8397	27,979	53,306
4	End of tether	8626	31,705	66,776

angle (at the exit of the tether deployer) could be determined to about 2–5 deg accuracy, dependent on the signal-to-noise ratio and the magnetometer accuracy. The out-of-plane angle remained virtually zero. The results show that the general trend and the hold-phase oscillation and the swing to the vertical are matching within the stated accuracy. The DIMAC data show a superimposed oscillation that is related to transversal waves around the direction to the end mass. A similar oscillation appeared in the matching simulation (see Sec. III.D.3).

The end shock at deployment completion occurs near  $\theta = 40$  deg. The release of Fotino ( $t = 9344$  s) and tether cut ( $t = 9364$  s) near  $\theta = 0$  deg. Release of the tether near the vertical is confirmed by a sudden disappearance of tether tension at  $t = 9364$  s (Sec. III.D.4) as well as by the measurements of NORAD's ground-based tracking system (now USSPACECOM). NORAD found a sudden change in Foton orbital elements and calculated the moment of divergence at  $t = 9364$  s with an altitude impact on Foton perigee of 1050 m at  $+61/-75$  m with 99.3% probability, using their special-perturbations model. This compares well with the momentum transfer that can be expected for a swing angle of 40 deg and a fully deployed tether released at the vertical if combined with an estimate of the Foton-M3 attitude control thruster effect. This Foton-M3 attitude control algorithm aimed to have the Foton body follow the tether, but to a maximum of  $\theta = 30$  deg. The tether effect of Foton perigee altitude can be determined to be  $950 \text{ m} \pm 3\%$ , plus  $150 \text{ m} \pm 25\%$  estimated for the Foton thruster contribution, or about  $1100 \text{ m} \pm 50 \text{ m}$  total. (The Foton thruster contribution was

determined from assuming a thrust level tuned to balance the tether torque above  $\theta = 30$  deg.)

Length and in-plane angle profiles can be combined to provide a convenient local-horizontal/local-vertical view of the tether deployment (Fig. 14). With the brake set to zero in most of the second stage, a higher velocity than nominal could be obtained, leading to a higher in-plane angle than foreseen. Although the release of the subsatellite was close to nominal in absolute distance and direction, the increased swing velocity and tether length imparted a greater  $\Delta V$  on the subsatellite and a steeper entry, considerably upstream from the nominal landing point.

Equation (2) was also used to reconstruct the deployment tension, which compares both qualitatively and quantitatively to the DIMAC measured levels (Figs. 10 and 15), providing further (rough) confirmation of the first stage length and the phase of the pendulum motion between the first and second stages. During the final part of the second stage, the curves diverge by almost 25%. The current understanding is that this divergence is partly due to tension model limitations, partly due to small deviations in deployment accelerations (compare with the result of the more advanced simulation in Fig. 15), and partly due to a low-frequency drift of the DIMAC sensors triggered by the continuous disturbance from the Foton thrusters in this period of deployment.

## 2. Deployer Performance Assessment

There are three main parameters that need to be assessed for in-flight qualification of the deployer hardware: in other words, to make sure that the deployer hardware (tether spool and barberpole brake) can be sufficiently characterized on the ground to allow reliable control of deployment in space. These parameters are taken from Eq. (1), the minimal deployment tension  $T_0$ , barberpole-brake friction coefficient  $f$ , and inertia multiplier  $I$  (Fig. 16).

The minimal deployment tension  $T_0$  (tether stickiness to the spool) is important in the early part of the first stage when gravity gradient is low, and the end-mass dynamics are determined by the end-mass inertia and the deceleration caused by this minimal friction level. The nominal level was 0.0085 N; the acceptable level for robust control of

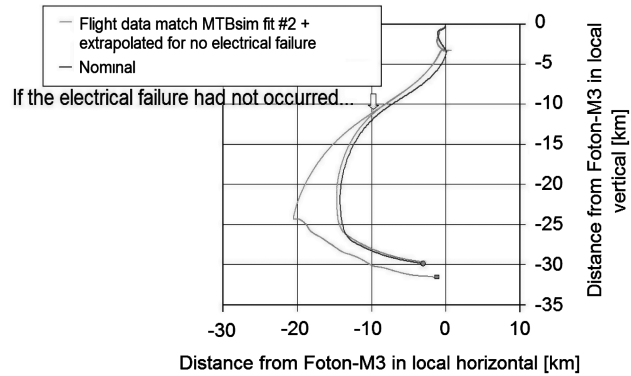
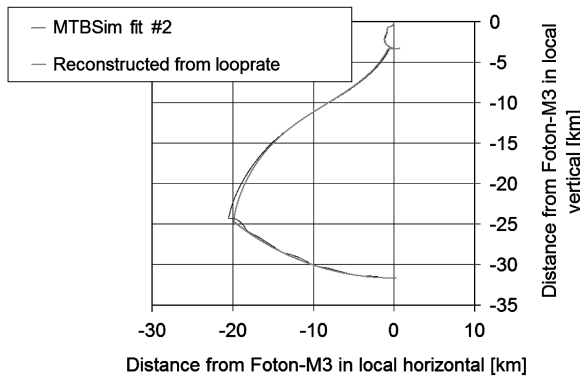


**Fig. 14** Matching of deployment trajectory (left), and mission match and extrapolated hypothetical deployment vs nominal in case no electrical failure had occurred (right).

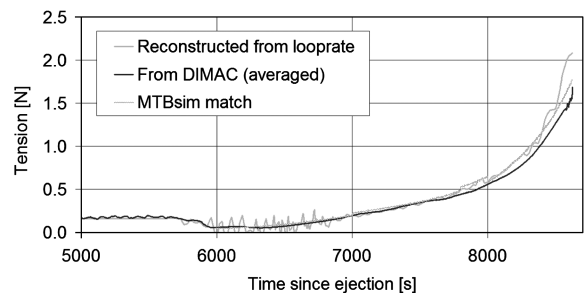
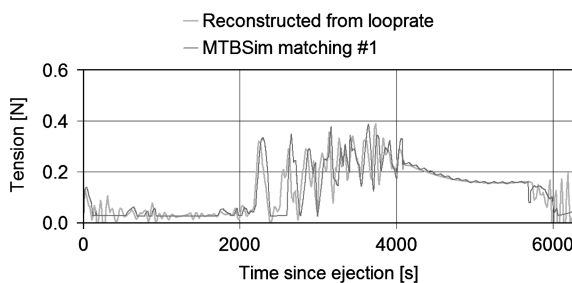


**Fig. 15** Matching of mission tension by simulation.

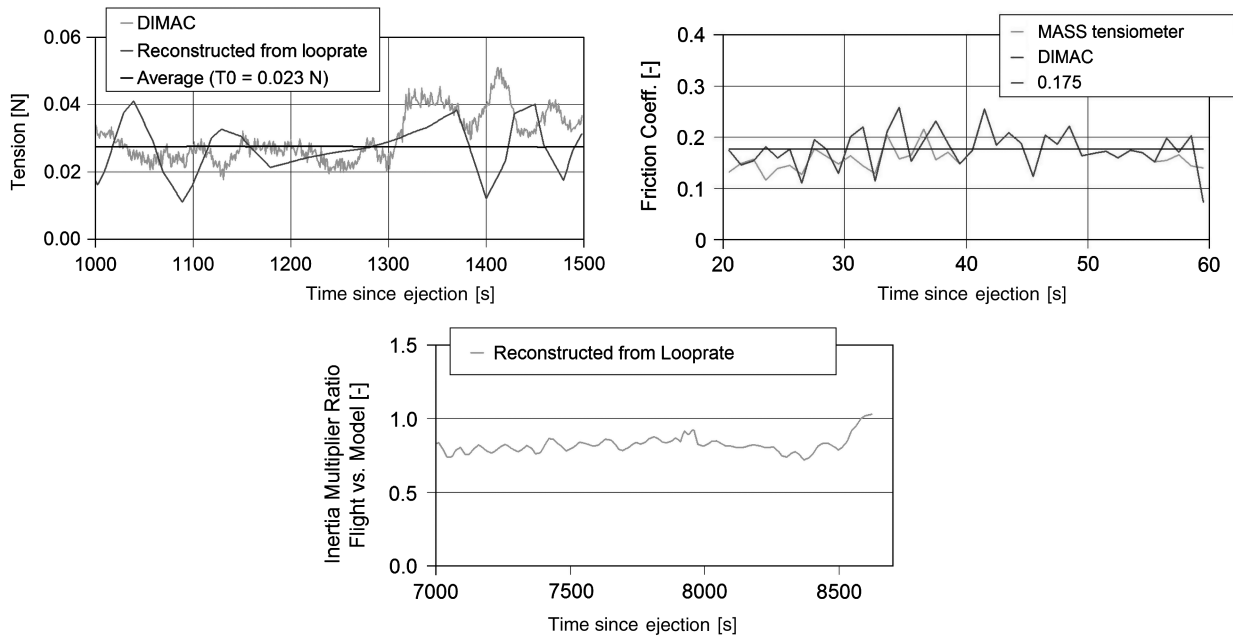


Fig. 16 Tether deployer performance expressed in the three main hardware parameters (see Sec. III.D.2).

deployment is 0.005 to 0.3 N. In flight, the level was quite high and ranged from 0.023 to 0.04 N.

The barberpole-brake friction coefficient  $f$  becomes important when the deployment needs to be controlled (for better precision) or actively decelerated. The nominal value is  $f = 0.2$ . A friction level below 0.12 would require a time-consuming amount of activation of the barberpole and would lead to a large number of wraps, decreasing brake effectiveness. A level above 0.3 can lead to controller resonance. A clean flight measurement was performed for the initial braking phase (Fig. 9) and resulted in a value of 0.175, close to nominal.

The inertia multiplier  $I$  represents (in a simplified manner) the dependency of spool unwinding tension on deployed length and deployment speed, including the effects of tether inertia, shock energy, compressibility of the spool, etc. The criticality of this parameter is not very high, as it is dominant in the high-speed deployment part of the second stage, in which gravity gradient is high and deployment is rather easy to control with the barberpole brake. The acceptable range is 2–20, with 8 as the nominal value. The zero brake setting during the final part of the second-stage setting allowed for a thorough assessment of this dynamic effect in the deployer tension model. Figure 16 shows the ratio between the value observed in flight and the preflight value. The result showed that the dynamic effect on tension in flight was matching the preflight model within 20%.

### 3. Tether Deployment Data Matching by Simulation

MTBSim is a simulator intended for reliable simulation of complete tether missions, including capsule reentry. MTBSim

approximates the tether by a large number of spring-mass elements (including viscosity effects during bouncing). Advanced environmental models and complex aspects are integrated into the tool [11]. For example, MTBSim includes a full tether hardware and controller software model. A deployment match is simply made by setting hardware parameters close to the flight measured levels. To account for the electronics failure around  $t = 6200$  s, the deployment controller is disabled at this moment and the brake is artificially set to zero position.

The deployment rate vs time could be matched within the accuracy of the available data (ranging between 5 cm/s and 1 m/s) by setting a single value for the hardware friction parameters, and an improved fit was obtained by varying some of the parameters by about 10% over the mission. Longitudinal waves were matched by increasing the tether viscosity with respect to expectations (stiffness was about nominal). Figures 14, 15, 17, and 18 show the matching results vs flight-measured/derived curves. Early matching attempts with a simplified controller model accurately reproduced the strong deceleration at  $t = 2200$  s, but, different from the flight data, deployment speed then recovered smoothly and no heavy and enduring velocity oscillations (such as in Fig. 15) and tension peaks (such as in Fig. 19, associated with transversal waves) were observed. When the software controller was then simulated in detail, including its low-pass-filter behavior, and the friction coefficient was finely adjusted, it was found that a controller-deployment resonance was created with resulting amplification of transversal waves, similar to that seen in flight (Fig. 20). The simulator tool thus seemed to be sufficiently realistic to be used as a diagnostic tool to study tendencies and dependencies. By changing simulation parameters, various ways were found to avoid occurrence of such unwelcome transversal

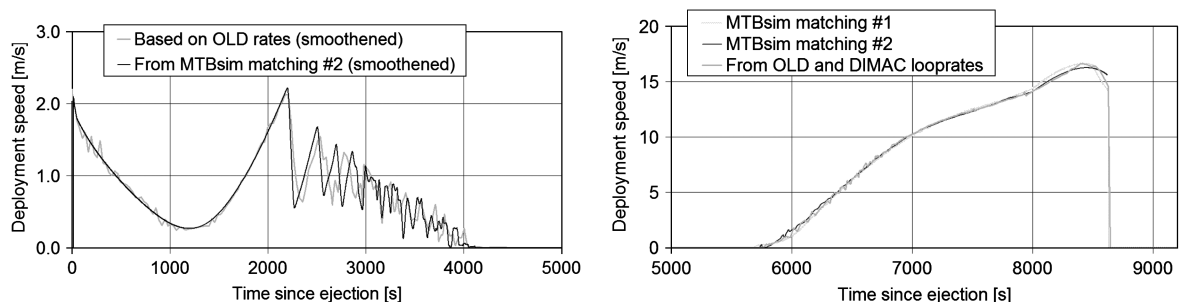


Fig. 17 Matching of deployment speed (first and second stages) by simulation including controller oscillations.

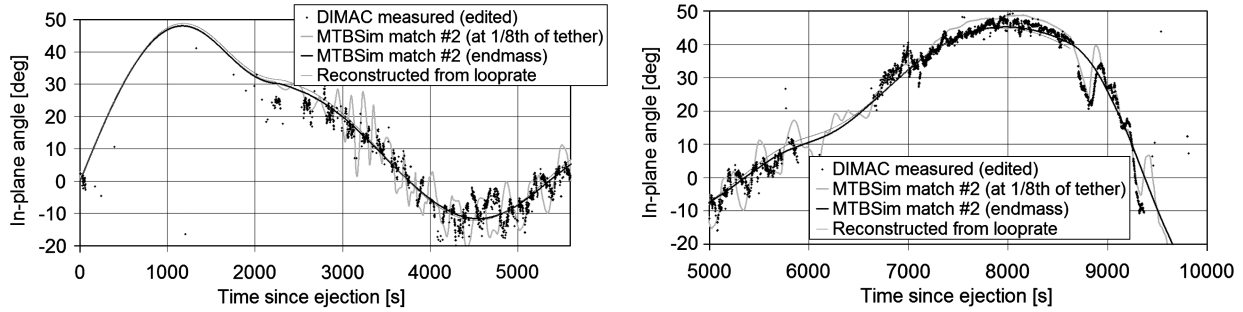


Fig. 18 Measurements and simulation of the tether in-plane angle with respect to the nadir.

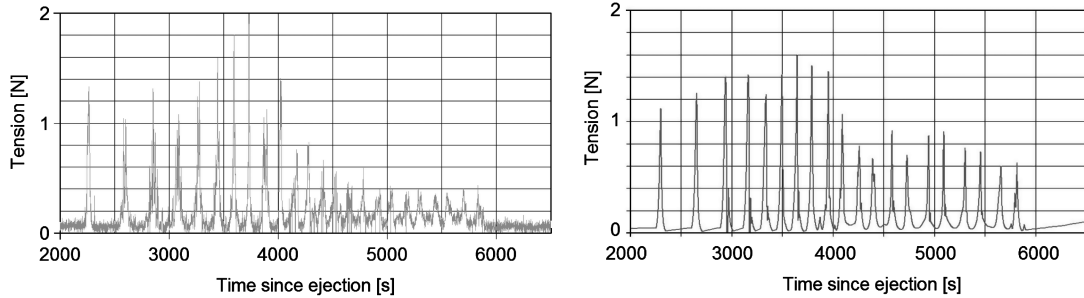


Fig. 19 Tension pulses from transversal waves during first stage and hold phase; flight data (left) and deployment-matching simulation (right).

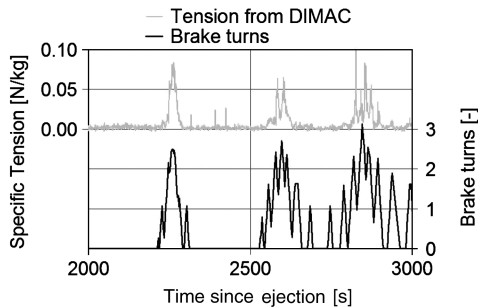


Fig. 20 Brake controller oscillations and effect on tension.

waves in future missions (Table 5). In subsequent figures, several matching results are included, covering various extreme simulator input cases, to provide an idea of the uncertainty associated with the matching result. Match 1 has a relatively low damping coefficient and stiffness, a relatively weak fit to deployment speed, and relatively little transversal wave excitation. Match 2 has a precise fit to deployment speed, a very high damping coefficient and stiffness, and heavy transversal wave excitation. The flight case lies somewhere in between.

Based on these results, positive conclusions could also be drawn with respect to the approach followed by the YES2 team for flight preparation. This approach includes a combination of Monte Carlo simulations for nominal deployment trajectory and controller development, real-time closed-loop deployment tests for flight hardware validation, and real-time hardware emulation for late-flight software testing. Some of the irregularities in the OLD pattern seen in the flight did not occur during the testing or preflight simulations. It was therefore found necessary to keep the flight algorithms more simple and more robust, as well as to include more detailed effects into the simulator used for algorithm development [11] (Table 5).

#### 4. Tether Oscillations

Tether bending during deployment is normal, due to Coriolis forces acting along the deploying tether. This is specifically true in early deployment if tension is low (about 3 cN in the case of YES2), if

deployment speed is high (YES2 maximum velocity was 16 m/s), and if tether mass is significant with respect to the end mass (YES2 end mass was 14 kg vs a 6 kg tether). Transversal waves are introduced if low-tension deployment is followed by abrupt braking (as occurred in YES2 at  $t = 2200$  s). Significant amplification of the waves after this shock was observed as a result of an unfortunate controller resonance with the deployment (Fig. 20). A second event introducing transversal waves was the end shock, as the tether was brought to an abrupt stop from a speed of 15 m/s. Transversal waves were recorded by the DIMAC instrument through their signature tension shocks (especially in the first stage), but also more directly by measurements of the angle under which the tether left Foton (Figs. 18 and 19).

The sudden stop of the tether at deployment completion occurred at a moment that the MASS/Fotino end mass was moving away from Foton at 15 m/s and led to a stretching of the tether of more than 100 m. As the tether relaxed, MASS/Fotino bounced back and came into a free orbital trajectory toward the local vertical below Foton. A kind of combined orbital bouncing/spring-mass oscillation was created (including also lateral and sound waves), causing repeated tension peaks of about 10 N. MTBSim reconstruction of the mission deployment matches this complex behavior qualitatively very well with proper selection of damping ( $\zeta = 0.14$ – $0.16$ , rather than 0.08 ground test) and stiffness ( $EA = 5000$ – $10,000$  N, as expected from ground tests) (Fig. 21). Here, the time reference is the time of completion of deployment and start of the swingback. The DIMAC data show the effect of tether cut around 740 s.

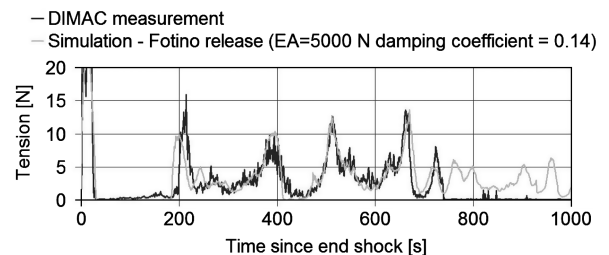


Fig. 21 Matching of spring-mass tension wave with transversal superimposed during swingback to vertical.

**Table 5** Analysis of problems occurring during YES2 and proposed solutions

Problem	Cause	Solution
Tether more sticky than expected, made it more difficult to control the deployment in the first stage.	Possibly due to 11 days of tether in thermal vacuum of space before deployment.	Test tether before and after full-scale exposure to representative environment, preferably also during such exposure.
Velocity filter overestimated the speed in the first minute after ejection, leading the controller to command additional braking, which lead to a decrease of velocity.	Software filter parameter not properly adjusted to real-flight condition.	1) Remove the particular filter feature (it concerns a feature to cover for the unlikely double-channel OLD failure case). 2) Adjust parameter based on YES2 mission data.
Software controller responds poorly to first transversal wave and amplifies the waves by resonance. Effect is decreased landing accuracy potential (by about 100 km).	Software velocity filter has a delay due to averaging and low-pass filtering, which can lead (in particular circumstances) to resonance between velocity and brake control.	1) Increase stepper motor speed by a factor two. 2) Decrease friction coefficient of brake pole (now it is sandblasted for higher friction). 3) Decrease tether stickiness (see preceding). 4) Optimize low-pass filter, taking this problem into account. 5) Optimize feedback gains, taking this problem into account.
Electrical failure in OLD-OBC interface, lead to open-loop control at end of second stage and bouncing of end mass on tether after completion, 1250 km landing error.	Failure on CPU board at the location of the OLD1 signal input (IRQ). The failure occurred before delivery of YES2 and was patched, but could not be sufficiently tested anymore. It was the patch that turned out faulty during flight.	Investigation of the CPU board failure, possibly selection of a more robust CPU board. More margins in testing timeline by earlier start of integration/testing phase.
Failure to receive signal from Fotino.	Possibly failure to release properly from MASS (due to possible end-mass rotation), heat shield failure, or beacon failure.	Confirm release: telemetry, simpler capsule (no heat shield sensors, focus on redundant beacon with robust monopole antennas). Avoid tether entanglement by center of mass position and attitude damping. More robust heat shield.

One event recorded during YES2 showed clear impact of a sound wave echoing back and forth through the tether several times: the end shock. Figure 22 is the tension profile of the end shock recorded at Fotino at the tether deployer end. The curious shape of the shock (rather than the typical sine pulse that MTBSim produces) is explained as follows. As the deploying tether is brought instantaneously to a standstill, at the site of the deployer in Fotino, from about  $v_0 = 15$  m/s, the remainder of the tether is still unaware of this event and traveling further. The information of the deployment stop travels down the full 31.7 km of tether with the speed of sound. As the deployment stop reaches any point in the tether at distance  $x$  from Fotino in  $\Delta t = x/a$  s, this point has moved  $v_0 \Delta t$ , and therefore the tether has built up an additional stretch by  $\Delta l = xv_0/a$ . Tension according to Hooke's law is  $\Delta T = EA \Delta l/l$ , and therefore  $T = EA x v_0/a/x = EA v_0/a$  and constant  $a$  can be obtained through  $a = 2l/P = 8.8$  km/s, where  $P$  is the observed time between shocks. This provides a quite precise expression for the tether stiffness from the tension measurement:  $EA = 2 \Delta T l / (P v_0) \sim 10,000$  N. After  $P/2$  s, the standstill reaches the other end of the tether. Fotino has significant inertia and pulls on the tether. A 15-m-long damping device (rip stitch [8]) mounted near Fotino activates and reduces the tension for about a second to  $\sim 6$  N. Then Fotino inertia restores and increases the tension such that the shock in the tether is reflected back to Fotino, where it is being measured  $P/2$  later as a further sudden rise. As Fotino slows down, the shock level drops until the reflection returns again, and 7 s later, a third and final time. Then Fotino has rebounded and the tether is slack. The maximum amplitude of  $\Delta T$  of about 37 N is somewhat larger, whereas the shock duration  $\frac{1}{2} P_{\text{shock}} = 14$  s is significantly shorter than would be obtained simulating a spring-mass system with infinite speed of sound for which

$$T = v_0 \sqrt{(Eam'/L)} = 33 \text{ N}$$

and

$$\frac{1}{2} P_{\text{shock}} = \frac{\pi}{\sqrt{(EA/m'L)}} = 24 \text{ s}$$

using  $m' = m_{\text{Fotino}} + 0.34 m_{\text{tether}}$ .<sup>§</sup> The following simulation (without damping, no ripstitch, and with lower  $EA$ ) for  $EA = 5000$  N,

$v_0 = 14$  m/s, and  $a = 10$  km/s (Fig. 22) illustrates the qualitative behavior.

#### 5. Comparison Between YES2 and the SEDS Deployments and Issues

YES2, albeit with independently developed hardware, employed similar technology as the SEDS-I and SEDS-II missions in, respectively, 1993 and 1994 and can be considered as an incremental mission (see Table B1, Appendix B). Whereas the SEDS-I mission was an open-loop deployment to a large angle, the SEDS-II tether featured a closed-loop deployment to the vertical at the full length of 20 km. Stabilization was obtained to within 4 deg. YES2 targeted a deployment to the vertical (at only 3.4 km), followed by a subsequent large-angle deployment at 30 km, both to be controlled in closed loop. The YES2 first stage final angle of 10 deg can be considered a control success, considering the challenging combination of high friction and low gravity gradient for such a short tether. The dynamic range of the second stage of YES2 was comparable with that of SEDS-I, although YES2 reached the greater velocity and length. The data from the DIMAC three-axis accelerometer, mounted close to the YES2 deployer, have been particularly powerful for reconstructing unique details of the deployment and dynamics. GPS/GLONASS navigation data promise to provide further in-plane angle confirmation. On the other hand, the SEDS end-mass dynamics sensors allowed for much more extensive analysis of end-mass attitude than has been possible with YES2 [33].

Data analysis of both YES2 and SEDS points to similar tether behavior, close to expected dynamics and well matched by simulations [26]. The mission performance deviates little from preflight analysis. Between SEDS and YES2, these deviations have some similarities and some differences.

The minimal deployment tension, due to stickiness and stiffness [34], has been displaying deviating values in both SEDS and YES2 missions. Similar to YES2, minimal deployment tension for SEDS-I was significantly higher than expected. In contrast, the SEDS-II mission showed a significantly lower level than nominal [35]. The SEDS team related the difference to the manufacturer [26] and suggested a relationship between low temperature and high stickiness, due to a surface finish on the fibers [34,36]. DSM High Performance Fibers, the Dyneema fiber manufacturer, applied the same identical antistatic finish to all YES2 tethers. Nevertheless, preflight testing in YES2 showed great differences between tethers that were subjected to different braiding angles and different postbraiding thermal and

<sup>§</sup>Private communication with S. A. Yost, February 2002.

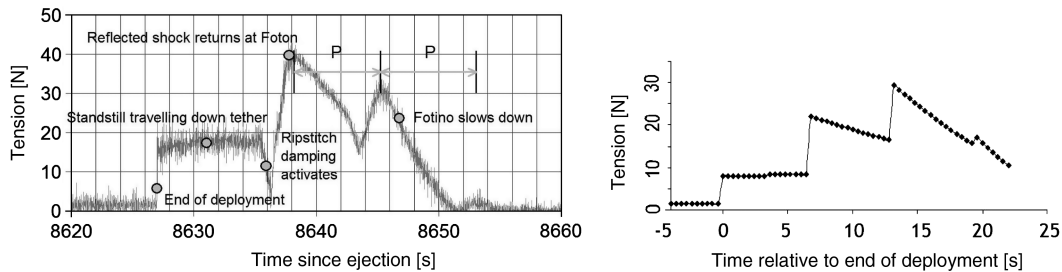


Fig. 22 Measured and simulated end shock showing echo in the tether.

prestretch treatments. Several tethers were even rejected for flight. Furthermore, these manufacturing differences have considerable effect on tether compressibility, stiffness, and shape memory.

The cause of the difference in behavior between ground tests and flight results for the same identical tether has been investigated by the YES2 team in postflight testing. Preliminary results point mostly to a settling of the tether due to thermal cycling. Early SEDS tests [37] showed that vacuum deployment testing produces qualitative differences in deployment in some cases. Deployment testing at MSFC in a representative thermal vacuum in fact produced estimates of the minimal deployment tension matching SEDS-II flight results [26,36]. At the low speeds of the first stage, atmospheric drag is not likely to be a major player, but a whole range of other factors could still be considered to be of impact. Candidates are lubrication by humidity, static charging effects on fibers or the tether as a whole, offgassing of the surface finish, chemical or mechanical changes to the fiber or the finish, and the thermomechanical settling effect currently hypothesized by the YES2 team. Further analysis is necessary and should result in recommendations for the required test environment.

Both missions experienced noise in deployment velocity. During the SEDS missions, stick-slip behavior of the deploying tether and scrubbing on the core flange [34] was suspected to be the cause. Noise was present from the time of ejection until velocity rose above about 5 m/s, with an amplitude of about 30% at 10 s averaged data [26]. Glaese et al. [38] relate stick-slip effects to the occurrence of sound waves. YES2 ground tests show a strong cyclic tendency in the minimal deployment tension, which could point to traditional stick slip through spring-mass effects. Spring-mass-induced stick slip did seem to occur near the end of the SEDS deployment when tether stiffness was relatively low and tension levels were high [26]. But in early deployment and at low tension, the tether would need to be orders of magnitude less stiff than test results indicate before sound waves or even spring-mass dynamics can explain stick slip. Also, the changes in deployment velocity are too rapid to be explained by an oscillating velocity of the end mass itself (i.e., through an alternating impact of friction and gravity-gradient).

A system capable of cyclic buffering and releasing tether must therefore be operating. End-mass angular oscillations may well be involved, but in YES2 they are too slow and have too small of an amplitude to explain the velocity noise fully. They may have been related to velocity noise in the early 100 s, but seem to have become insignificant (or more indirect) afterward. However, transversal waves or bulging or shape-memory coils in the tether can act to extract and buffer the slipping tether. The YES2 deployment velocity was rather smooth until a large braking action started oscillations at 2200 s. From inspection of the relationship between tension, brake control, and OLD patterns, these oscillations seem to be maintained and amplified by a controller resonance with the velocity. Confirmation seems to come from MTBSim (Sec. III.D.3), with which such oscillations were made visible, even when no end-mass dynamics and no sound waves were simulated, once the controller details were implemented.

The YES2 controller parameters should be adjusted to avoid this resonance. As a potential solution, a large control interval with low-pass filter (0.02 Hz) was applied on SEDS-II, because noisy OLD output was expected in advance [39]. In addition, to dampen

transversal and end-mass modes on SEDS, a heat-shrink tube was added around the tether fixture [34] (longitudinal damping is provided through the barberpole-brake principle). A system such as the absorptive tether implemented on the first YES is to be recommended for a future mission [13].

As far as matching of the deployment is concerned, Lorenzini et al. [26] conclude for the SEDS case that the tension model (1) is suitable for mission planning yet is too simple for a good fit, although an impressive qualitative comparison can be made if noise models are used. For example, in the SEDS-I early deployment, a nearly constant deceleration was observed that could not be well explained. A complex tension dependency was expected [38]. Somewhat in contrast, the match achieved for YES2 appears to be rather exact and no particular problems or challenges have arisen in achieving it. For YES2, a precise match could be obtained using Eq. (1), which was further improved when the minimum deployment tension  $T_0$  was made linearly dependent on velocity below a speed of 1 m/s. The final bounce was reproduced to such an extent that tether properties such as stiffness and damping could be derived. The bounce tension development is similar to that seen in SEDS-I (a simulator match of the SEDS-I final bounce was not made [38]).

#### 6. Fate of Fotino and the SpaceMail Potential

A deployment-matching simulation using the MTBSim mission simulator (see Sec. III.D.3) with nominal Fotino release time was used to determine the most likely actual landing site of Fotino. An error ellipse around this was determined based on the identified error sources, including a  $150 \times 20$  km uncertainty due to atmospheric density/horizontal wind uncertainty during entry, capsule mass and drag coefficient uncertainty (due to ablation), Fotino release delay, and model/matching errors. The simulations show that reentry conditions for Fotino would have just fallen within the nominal windows for entry angle, heat flux, and angular rate (Fig. 23).

Figure 24 shows the resulting reconstructed landing area, about 1250 km upstream of the nominal landing point. The area dimensions are about  $250 \times 30$  km, in the border region of Kazakhstan, Uzbekistan, and Turkmenistan.

There is no confirmation yet that Fotino was delivered to the ground as intended. However, sufficient data were gathered to assess the potential of the YES2 SpaceMail system as developed and as flown, for future applications.

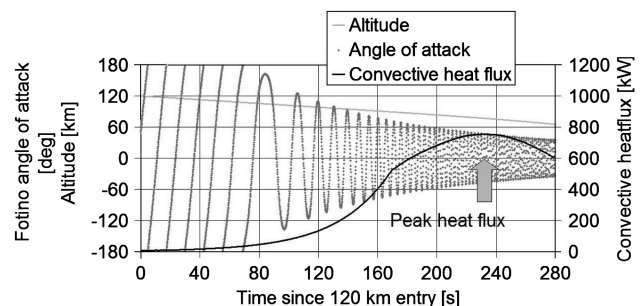


Fig. 23 Fotino conditions during entry.





Fig. 24 Reconstructed Fotino landing area (image: Google Earth).

Data have also allowed the understanding that the Fotino trajectory insertion error can be attributed almost fully to the interface electronics power failure occurring around  $t = 6200$  s. When the same deployment-matching simulation is performed without (artificial) introduction of the electrical failure at  $t = 6200$ , deployment recovers smoothly from the troubled first stage and landing would still be within the nominal landing ellipse, about 150 km downstream from the nominal landing site (Figs. 14 and 25), a performance comparable with conventional retrorocket reentry of ballistic lightweight capsules. Figure 25 shows the extrapolated landing site if the filter resonance problem would be resolved (reducing the transversal waves), nearly coinciding with the nominal landing point, and the (unofficial) recovery team location at the time of the expected landing is also visible.

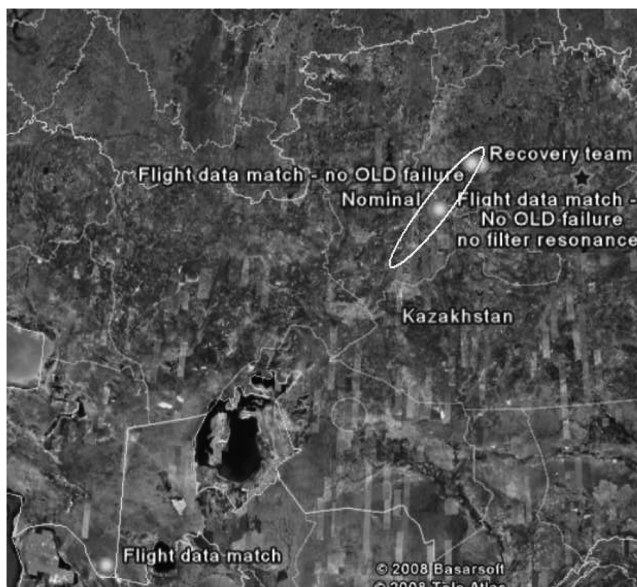


Fig. 25 Nominal landing area including, the hypothetical landing site of Fotino resulting from extrapolation of mission data assuming no electrical failure at  $t = 6260$  s (image: Google Earth). The star indicates the Kazakh capital, Astana.

Other problems were identified and have to be fixed, but they would have had only secondary impact on the mission result. They are listed with their proposed, often simple and straightforward, solutions in Table 5.

#### IV. Conclusions

In September 2007, the YES2 experiment deployed a 31.7 km tether in space for the purpose of a tethered SpaceMail reentry demonstration, for the first time featuring a two-stage deployment and release optimized for accurate entry and paying particular attention to safety with respect to the deployment platform.

A set of data was obtained allowing for cross-validation of nearly all features of the mission. The data from a precise three-axis accelerometer situated close to the deployer turned out to be particularly informative. Such a sensor is recommended for future missions. Apart from length and velocity, the in-plane dynamics could be derived and studied. From the analysis, it could be confirmed that the tether deployer and tether safety features behaved nominally, with the exception of the minimal deployment tension, which had increased significantly with respect to preflight conditions. The increase is suspected to be a result of thermomechanical settling of the spool. Tether properties and wave dynamics could also be studied and the measured mission dynamics could be satisfactorily matched by simulation. The deployment was reconstructed with an accuracy of 20 m for the first stage of 3.4 km and about 100 m for the full length of 31.7 km.

The YES2 deployment itself was mostly nominal, but ended in an offnominal manner, after failure of sensor-to-processor interface electronics. For this reason, the capsule is thought to have landed 1250 km upstream of the nominal landing point. The potential for SpaceMail performance for the hardware as flown (in absence of the electrical failure) could, however, still be quantified and found to be in accordance with expectations. About 200 km landing-site accuracy is possible for a ballistic entry with the YES2 system, comparable with conventional retrorocket solutions.

As postmission data analysis shows there are no major hurdles, the YES2 system, simulation, and test facilities can be used with only small modifications for future reentry missions and early tether applications. The tether unwinding behavior, tether oscillation dynamics, and controller behavior have been studied and, as a result, the required modifications have been defined. Ground testing should have sufficient focus on understanding the variables affecting the minimal deployment tension and include at least an offgassing and a realistic thermal history. The algorithm for determining the length from loop counts can be made more robust by simplifying it. To determine the controller robustness before flight, the simulations performed as part of the sensitivity analysis should include realistic models of not only tether and deployer hardware, but also of software and velocity filter. The end-mass stability would need to be better secured against occurrence of tether slackness by inclusion of a dissipative damping system around the tether near the end mass and possibly some basic attitude control. A more robust capsule with a redundant beacon system is recommended.

The results of the SEDS missions have shown to be reproducible, even with the educational approach of YES2, underlining the strength of the spool-and-barberpole deployment concept. A sequel mission must be fully successful and would only then be beneficial to the development of tether systems aimed to eventually obtain a sustainable space transportation system.

#### Appendix A: YES2 Deployment Parameters and Data Sources

Tables A1–A5 provide an overview of the various mission parameters and the data sources used for their estimation. A description of the sensors is found in Sec. III.B and in more detail in [8,27,28,30].

**Table A1 Overview of mission parameters and results**

Mission parameter	Nominal value	Acceptable range	Result
Ejection speed	2.2 m/s after tie-downs	1.2–3 m/s	Nominal: 2.2 m/s after tie-downs
Subsatellite initial dynamics around center of mass	10 deg/s initially	—	Nominal: 1.55 deg/s initially
Subsatellite continued dynamics around center of mass	Max 90 deg amplitude oscillation	Max 90 deg amplitude oscillation	Offnominal: subsatellite appears to be tumbling as a result of slackness
Deployment speed $t < 6260$ s	0–6 m/s	—	Acceptable: initially too much braking, due to temporary bad filtering
First-stage length profile	—	—	Nominal
First-stage length	3390 m	3100–3700 m	Nominal: 3380 m
Deployment speed 6260–8626 s	5–13 m/s	—	Offnominal: 5–16 m/s, due to OLD registration failure
Second-stage length profile	30,000 m	29,000–31,000 m	Offnominal: 31,700 m, due to OLD registration failure
In-plane angle	0–50 deg	—	Acceptable
Out-of-plane angle	0 deg	5 deg	Nominal: 0 deg
Fotino release	Release at $t = 9364$ s, 6 deg before vertical, entry angle 1.4 deg	20 s release error, 0.2 deg entry angle error	Acceptable: release $t = 9364$ s, entry angle 1.5 deg
Fotino landing site	Near Tasty Taldy, 66.3E 50.6N, Kazakhstan	200 km error	Offnominal: ~1250 km upstream, approx 55.7E 41.6N
Deployer performance	See Eq. (1)	About a factor 3, and 50% on friction	Nominal: friction (10–15%), dynamic effect (15%); acceptable: stickiness (factor 2.7–4)
Tether properties	$EA = 5000$ , $a = 10$ km/s, $\zeta = 0.08$	About a factor 3	Nominal: $EA = 5000$ –10,000, $a = 8.8$ km/s, $\zeta = 0.14$ –0.16

**Table A2 Data sources used: ejection and end mass dynamics**

Data sources	Description	Attainable accuracy
<i>Ejection speed</i>		
OLD	Initial OLD rate	0.1 m/s
MASS tensiometer plus OLD	Integration of acceleration derived from MASS tensiometer, fit to OLD rate development	0.1 m/s
DIMAC plus OLD	Integration of DIMAC accelerations, fit to OLD rate development	0.1 m/s
<i>Subsatellite initial dynamics around center of mass</i>		
MASS gyroscope	Direct measurement (1 axis)	0.2 deg/s
<i>Subsatellite continued dynamics around center of mass</i>		
MASS magnetometers	3-axis derivatives	1 deg/s
MTBSim Simulator + DIMAC	Simulation using tension data fit to initial MASS data	—

**Table A3 Data sources used: deployment length and speed**

Data sources	Description	Attainable accuracy
<i>Deployment speed <math>t &lt; 6260</math> s</i>		
OLD	Rate data	~0.05 cm/s
DIMAC (plus OLD)	Confirmation by comparison of DIMAC derived tension to OLD reconstructed tension [Eq. (1)]	1%
<i>First-stage length profile</i>		
OLD	Loop count	20 m
<i>First-stage length</i>		
OLD (plus statistical analysis)	Loop count, time interval/statistical analysis to estimate error	20 m
DIMAC	Gravity-gradient tension from DIMAC for hanging tether	~100 m
<i>Deployment speed 6260–8626 s</i>		
DIMAC	Spectrograph rate profile	0.2–0.7 m/s
OLD	Rate data (interpolated over last 400 s)	1 m/s
<i>Second-stage length profile</i>		
DIMAC	Integration of spectrograph rate profile	100 m
DIMAC	3 transition points in winding turns per cycle setting from spectrograph, end of deployment from tension spike	100 m
OLD	Reconstruction using rate data	~200 m

**Table A4 Data sources used: deployment angle and capsule trajectory**

Data sources	Description	Attainable accuracy
<i>In-plane angle</i>		
OLD (plusDIMAC, MTBSim)	Reconstruction using rate data with Eq. (2) or MTBSim. Better if amended with DIMAC spectrograph rate data.	2 deg
DIMAC	From ratio of <i>x</i> -axis and <i>y</i> -axis measurements combined with Foton orientation from magnetometer and horizon sensor.	5 deg
GPS	Determine vector to system center of mass. Not performed yet.	~1–5 deg (estimate)
<i>Out-of-plane angle</i>		
DIMAC	<i>z</i> -axis acceleration	~1 deg
<i>Fotino release</i>		
OLD plus DIMAC plus MTBSim simulator	Continuation of dynamics after deployment completion by simulation. Measured tension drop at tether cut.	1%
NORAD ground-based radar	NORAD measurement of Foton orbit after release evidencing momentum transfer.	6%
<i>Fotino landing site</i>		
Fotino Beacon	Argos Beacon signal (failed)	350 m
OLD plus DIMAC plus MTBSim simulator	Simulation based on match of DIMAC tension profile during swing.	125 km

**Table A5 Data sources used: deployment and tether properties**

Data sources	Description	Attainable accuracy
<i>Deployer performance</i>		
DIMAC	Derived tension	10–25%
OLD plus DIMAC	Deployment reconstruction	10–25%
OLD plus DIMAC plus MTBSim Simulator	Deployment matching	10–25%
MASS tensiometer	Brake friction coefficient	~15%
<i>Tether properties</i>		
DIMAC	Derived tension	—

## Appendix B: Comparison Between SEDS and YES2 Missions

**Table B1 Characteristics of the SEDS missions vs the YES2 deployment stages**

	SEDS-1	SEDS-2	YES2 stage 1	YES2 stage 2
Year	1993	1994	2007	
Tether diameter, mm	0.75	0.75	0.5	
Tether linear density, kg/m	0.33	0.33	0.18	
End mass, kg	26	26	14	
Ejection velocity, m/s	1.64	1.6	2.2	
Control	Open loop	Closed loop	Closed loop	Closed/(open) loop
Control input	—	2 optical loop sensors	3 optical loop sensors	
Control output	Wraps around capstan	Wraps around capstan	Wraps around capstan	
Control interval, s	—	8	2	
Length target/obtained, km	20/20	19.75/19.78	3.38/3.39	30.1/31.7
Final velocity target/obtained, m/s	0/7	0/0.02	0/0.00	0/15
Angle target/obtained, deg	—/53	0/4	0/10	40/45
Minimum tension expected/observed, N	0.01/0.035	0.03/0.015	0.008/0.03	
Maximum tension, N	7	2.5	~1	40
Maximum speed target/obtained, m/s	10.6/12.8	5.6/5.9	2.2/2.2	13/16
Length/velocity data	YES	YES	YES	YES
In-plane angle data	NO	Ground radar	YES	YES
Tension data	Tether exit, end mass	Tether exit, end mass	At end mass, deployer acceleration	Deployer acceleration
End-mass dynamics data	Yes	Yes	Partial	No

### Acknowledgments

This work was performed under ESA contract 22154/08/NL/PA “YES2 Flight Analysis and Definition for a Re-Flight.” For this paper, thanks go to Christophe and Tom from Redshift for providing direct measurement of acceleration (DIMAC) results and to Nikolay Smirnov and Alexey Malashin for their analysis of the final shock and echo phenomenon observed at end of the YES2 tether deployment. For YES2, thanks go to ESA Education Office and the Manned Spaceflight Directorate, the tens of participating universities around Europe and beyond and the hundreds of students from 25 countries that made this project possible.

### References

- [1] Carroll, J. A., “SEDS Deployer Design and Flight Performance,” AIAA Paper 93-4764, 1993.
- [2] McCoy, J. E., O’Neil, Co., Stanley, J., Settecerrri, T., Grossi, M.D., Estes, R.D., et al., “Plasma Motor Generator Flight Experiment Results,” *Fourth International Conference on Tethers in Space*, Science and Technology Corp., Hampton, VA, 10–14 Apr. 1995, pp. 57–82.
- [3] Levin, E. M., *Dynamic Analysis of Space Tether Missions*, Advances in the Astronautical Sciences, Vol. 126, Univelt, San Diego, CA, 2007.
- [4] Dobrowolny, M., and Stone, N. H., “A Technical Overview of TSS-1: The First Tethered Satellite System Mission,” *Il Nuovo Cimento C*, Vol. 17, No. 1, Feb. 1994, pp. 1–12.

- doi:10.1007/BF02506678
- [5] De Pascale, F., and Kruijff, M., "Fotino: Design, Manufacturing, Testing of the Capsule for the Second Young Engineers Satellite," International Astronautical Congress Paper 06-E1.1.05, 2006.
  - [6] Asma, C., De Pascale, F., and Kruijff, M., "Heatshield Qualification for the SpaceMail Re-Entry Capsule 'Fotino' in the VKI Plasmatron," AIAA Paper 2008-6561, 2008.
  - [7] Ockels W. J., van der Heide, E. J., and Kruijff, M., "Space Mail and Tethers, Sample Return Capability for Space Station Alpha," International Astronautical Federation, Paper 95-T.4.10, 1995.
  - [8] Kruijff, M., Hambloch, P., van der Heide, E. J., and Stelzer, M., "The Second Young Engineers' Satellite, YES2," International Astronautical Congress Paper 07-D2.3.04, 2007.
  - [9] Kruijff, M., van der Heide, E. J., Stelzer, M., Ockels, W. J., and Gill, E., "First Mission Results of the YES2 Tethered SpaceMail Experiment," AIAA Paper 2008-7385, 2008.
  - [10] Kruijff, M., and van der Heide, E. J., "Qualification and In-Flight Demonstration of a European Tether Deployment System on YES2," *Acta Astronautica*, Vol. 64, Nos. 9–10, 2009, pp. 882–905. doi:10.1016/j.actaastro.2008.10.014
  - [11] Kruijff, M., van der Heide, E. J., and Stelzer, M., "Applicability of Tether Deployment Simulation and Tests Based on YES2 Flight Data," AIAA Paper 2008-7036, 2008.
  - [12] Kruijff, M., The Young Engineers' Satellite, "Flight Results and Critical Analysis of a Super-Fast Hands-On Project," International Astronautical Federation, Paper 99-P.1.04, 1999.
  - [13] Kruijff, M., and van der Heide, E. J., "The YES Satellite: A Tethered Momentum Transfer in the GTO Orbit," *Proceedings of the Tether Technology Interchange Meeting*, CP-1998-206900, NASA Jan. 1998.
  - [14] Gavira, J., Rozemeijer, H., Muencheberg, S., "The Tether System Experiment," ESA/European Space Research and Technology Centre, Bulletin 102, Noordwijk, The Netherlands, 2000.
  - [15] Menon, C., Kruijff, M., and Vavouliotis, A., "Design and Testing of a Space Mechanism for Tether Deployment," *Journal of Spacecraft and Rockets*, Vol. 44, No. 4, July–Aug. 2007, pp. 927–939. doi:10.2514/1.23454
  - [16] Kruijff, M., and van der Heide, E. J., "Integrated Test Rig for Tether Hardware, Real-Time Simulator and Control Algorithms: Robust Momentum Transfer Validated," *Space Technology and Applications International Forum 2001*, CP552, American Inst. of Physics, Melville, NY, 2001.
  - [17] "European Users Guide to Low Gravity Platforms," ESA, Rept. UIC-ESA-UM-0001, Paris, 2005.
  - [18] Kruijff, M., and van der Heide, E. J., "YES2 Education and Outreach," International Astronautical Congress Paper 03-P.P.01, 2003.
  - [19] Willekens, P., Van Dijk, A., Kruijff, M., Van der Heide, E. J., "Young Engineers' Satellite, Educational Demonstration of SpaceMail," *On Station*, No. 17, Aug. 2004.
  - [20] Hyslop, A., Kruijff, M., Menon, C., "Simulating Space Tether Deployment on Earth for the YES2 Satellite," *56th International Astronautical Congress*, International Astronautical Federation, Paris, 2005, pp. 297–310; also International Astronautical Federation Paper IAC-05-A2.1.09
  - [21] Hambloch, P., De Pascale, F., and Kruijff, M., "ALBATROs: A Space System Engineering Tool," International Astronautical Congress Paper 07-D5.1.05, 2007.
  - [22] Hausmann, G., De Pascale, F., Kruijff, M., and Mironov, M., "Design, Development and Testing of a Compact Lightweight Capsule Recovery System," International Astronautical Congress Paper 08-D2.3.5, 2008.
  - [23] Williams, P., Hyslop, A., and Kruijff, M., "Deployment Control for the YES2 Tether-Assisted Reentry Mission," *Advances in the Astronautical Sciences*, Vol. 123, No. 2, 2006, pp. 1101–1120. also American Astronautical Society Paper 05-322, 2005.
  - [24] Spiliotopoulos, I., Kruijff, M., and Mirmont, M., "Development and Flight Results of a PC104/QNX-Based Onboard Computer and Software for the YES2 Tether Experiment," *Proceedings of the Small Satellite Systems and Services (4S) Symposium* [CD-ROM], SP660, ESA/European Space Research and Technology Centre, Noordwijk, The Netherlands, 2008.
  - [25] Graczyk, R., Kruijff, M., and Spiliotopoulos, I., "Design and Qualification of a Smallsat Stepper Motor Driver, Flight Results On-Board the YES2 Satellite," *Proceedings of the Small Satellite Systems and Services (4S) Symposium* [CD-ROM], SP660, European Space Research and Technology Centre, Noordwijk, The Netherlands, 2008.
  - [26] Lorenzini, E. C., Mowery, D. K., and Rupp, C. C., "SEDS-II Deployment Control Law and Mission Design," *Proceedings of the Fourth International Conference on Tethers in Space*, Science and Technology Corp., Hampton, VA, Apr. 1995, pp. 669–684.
  - [27] Beuselinck, T., Bavinckhove C. Van, Abrashkin, V. A., and Sazonov, V. V., "Attitude Motion of the Foton-M3 Spacecraft and Quasi-Steady Accelerations on Its Board," *Proceedings of SPEXP-2008* [CD-ROM], Inst. of Cosmonautics, Volga Branch, Samara, Russia, 2008 (in Russian).
  - [28] Castillejo, G., Cichocki, A., and Burla, M., "Development, Test and Flight Results of the RF Systems for the YES2 Tether Experiment," International Astronautical Congress Paper 08-E2.3.6, 2008.
  - [29] Belokonov, I. V., Kudriavtsev, I. A., Kramlikh, A. V., and Potudinsky, A. A., "The Results of the Navigating Experiment During the SC 'Foton-M3' Flight," *Proceedings of SPEXP-2008* [CD-ROM], Inst. of Cosmonautics, Volga Branch, Samara, Russia, 2008 (in Russian).
  - [30] Belokonov, I., "Improvement of Navigational Tracking Instrumentation and Methods of Tether System Deployment on an Example Of Experiment YES2 on Space Vehicle Foton-M3," International Astronautical Congress Paper 08-B2.1.10, 2008.
  - [31] Hyslop, A., van der Heide, E., Stelzer, M., Kruijff, M., Bonnal, C., Talbot, C., et al., "Designing a Micro-Launcher with Tethered Upper Stage," International Astronautical Congress Paper 06-D2.3.03, 2006.
  - [32] van der Heide, E. J., and Kruijff, M., "StarTrack, a Swinging Tether Assisted Re-Entry for the International Space Station," ESA/European Space Research and Technology Centre, Working Paper 1883, Noordwijk, The Netherlands, Mar. 1996.
  - [33] Stadler, J. H., "SEDS End Mass Payload Magnetometer Engineering Performance and Rotational Data Analysis Results," *Proceedings of the Fourth International Conference on Tethers in Space*, Science and Technology Corp., Hampton, VA, Apr. 1995, pp. 613–626.
  - [34] Carroll, J. A., and Oldson, J. C., "SEDS Characteristics and Capabilities," *Proceedings of the Fourth International Conference on Tethers in Space*, 1995, pp. 1079–1090.
  - [35] Bortolami, S. B., Lorenzini, E. C., Rupp, C. C., and Angrilli, F., "Control Law for the Deployment of SEDS II," *Advances in the Astronautical Sciences*, Vol. 85, 1993, pp. 733–748; also American Astronautical Society Paper AAS 93-706.
  - [36] Wallace, B. K., "SEDS Tether Deployment Ground Tests," *Proceedings of the Fourth International Conference on Tethers in Space*, Science and Technology Corp., Hampton, VA, Apr. 1995, pp. 653–668.
  - [37] Carroll, J. A., "The Small Expendable Deployment System (SEDS)," *Space Tethers for Science in the Space Station Era*, Società Italiana di Fisica, Bologna, Italy, 1988, pp. 43–50.
  - [38] Glaese, J., Issa, R., and Lakshmanan, P., "Comparison of SEDS-1 Pre-Flight Simulations and Flight Data," AIAA Space Programs and Technologies Conference, AIAA Paper 93-4766, 1993.
  - [39] Lorenzini, E. C., Bortolami, S. B., Rupp, C. C., and Angrilli, F., "Control and Flight Performance of Tethered Satellite Small Expendable Deployment System-II," *Journal of Guidance, Control, and Dynamics*, Vol. 19, No. 5, 1996, pp. 1148–1156. doi:10.2514/3.21757

J. Martin  
Associate Editor